Magnon-assisted dynamics of a hole doped in a cuprate superconductor

I. J. Hamad and L. O. Manuel
Instituto de Física Rosario (CONICET) and Facultad de Ciencias Exactas, Ingeniería y Agrimensura, Universidad Nacional de Rosario, Bulevar 27 de Febrero 210 bis, 2000 Rosario, Argentina

A. A. Aligia
Centro Atómico Bariloche and Instituto Balseiro, Comisión Nacional de Energía Atómica, CONICET, 8400 Bariloche, Argentina

(Received 29 January 2021; revised 30 March 2021; accepted 1 April 2021; published 14 April 2021)

We calculate the quasiparticle dispersion and spectral weight of the quasiparticle that results when a hole is added to an antiferromagnetically ordered CuO_2 plane of a cuprate superconductor. We also calculate the magnon contribution to the quasiparticle spectral function. We start from a multiband model for the cuprates considered previously [Ebrahimnejad *et al.*, Nat. Phys. **10**, 951 (2014)]. We map this model and the operator for creation of an O hole to an effective one-band generalized t-J model, without free parameters. The effective model is solved using the state-of-the-art self-consistent Born approximation. Our results reproduce all the main features of experiments. They also reproduce qualitatively the dispersion of the multiband model, giving better results for the intensity near wave vector (π,π), in comparison with the experiments. In contrast to what was claimed in Ebrahimnejad *et al.*, we find that spin fluctuations play an essential role in the dynamics of the quasiparticle and hence in both its weight and dispersion.

DOI: 10.1103/PhysRevB.103.144510

I. INTRODUCTION

More than three decades after the discovery of high-temperature superconductors, the issue of the appropriate microscopic minimal model that correctly describes the low-energy physics is still debated. There is, however, a consensus on the validity of the three-band model H_{3b} for describing the physics of the cuprates at energies below $\sim$1 eV, where the three bands come from two O $2p_\sigma$ orbitals (those pointing in the direction of the nearest Cu sites) and one Cu $3d_{x^2-y^2}$ orbital [1,2]. At higher energies other orbitals should be considered [3–7]. Other models used to describe the cuprates are the spin-fermion model H_{sf} [8], obtained from H_{3b} after eliminating the Cu-O hopping by means of a canonical transformation (only the d^9 configuration of Cu is retained, represented by a spin 1/2, which interacts with the fermions of both O bands) [9,10], and the generalized t-J model H_{GtJ} [11,12], which consists of holes moving in a background of Cu 1/2 spins with antiferromagnetic exchange J, nearest-neighbor hopping t, and additional terms of smaller magnitude.

H_{GtJ} is derived as a low-energy effective one band model for H_{3b} or H_{sf} [12–14], assuming that the low-energy part of the multiband models is dominated by Zhang-Rice singlets (ZRSs) [11], which in H_{sf} consist of singlets formed between the spin of a copper atom and the spin of the hole residing in a linear combination L of four ligand oxygen orbitals around the copper atom [11,12]. In H_{3b}, in which charge fluctuations are allowed, the ZRS also includes states with two holes in the Cu $3d_{x^2-y^2}$ orbital and in the O L orbital [14,15]. The proposal of Zhang and Rice has initiated a debate about the validity of a one-band model that continues at present [8,16–28]. This issue is of central importance since models similar to the t-J model were used to explain many properties of the cuprates [29,30], including superconductivity [31–33].

An important probe for the models is the spectral function of a single hole doped on the parent half-filled compounds, whose quasiparticle (QP) dispersion relation is directly measured in angle-resolved photoemission (ARPES) experiments [34,35]. The nature of this QP has been extensively discussed [36–39]. Experimental evidence shows that this doped hole resides mainly on the O $2p_\sigma$ orbitals [40–42]. Naively, one might expect that this fact is a serious problem for H_{GtJ} since O holes are absent in the model. However, mapping appropriately the corresponding operators, Cu and O photoemission spectra can be calculated with both H_{sf} [10] and H_{GtJ} [43]. Nevertheless, while the experimental dispersion observed in $Sr_2CuO_2Cl_2$ [34] has been fit using H_{GtJ}, an unsatisfactory aspect is that the "bare" t-J model with only nearest-neighbor hopping t was unable to explain the observed dispersion, and *ad hoc* hopping to second- and third-nearest neighbors was included [44–47].

In Ref. [23], the QP dispersion $E_{QP}(\mathbf{k})$ and its intensity $Z_{QP}(\mathbf{k})$ for adding an O hole in an undoped CuO_2 plane were calculated, using H_{sf} solved with an approximate variational method using realistic parameters. The dispersion obtained agrees with experiment. However, the reported intensity increases as k moves from $(\frac{\pi}{2},\frac{\pi}{2})$ to (π,π), in contrast to experiment. The main claim of the mentioned reference was that background spin fluctuations play no role in the dynamics of the hole, and only local spin fluctuations around the hole are important.

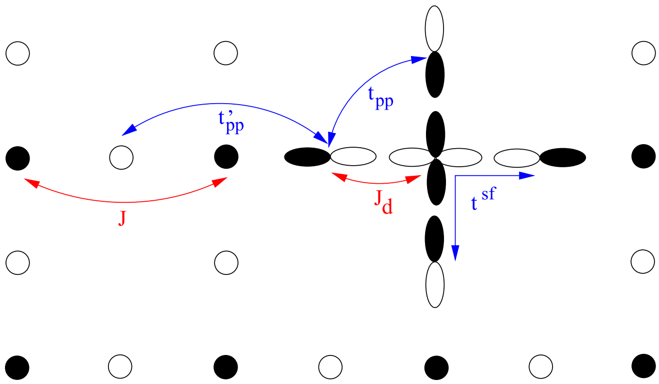

FIG. 1. Structure of the CuO_2 planes and sketch of the parameters of the three-band spin fermion model [Eq. (1)]. Solid (empty) circles represent Cu (O) sites.

In this work we map the H_{sf} used in Ref. [23] to an H_{GtJ} without adjustable parameters, extending to Z_{QP} the procedure we used before for T-CuO [28]. The resulting H_{GtJ} is solved using the state-of-the-art self-consistent Born approximation (SCBA). We obtain results in agreement with experiment for both E_{QP} and Z_{QP}. We also calculate the hole's spectral function by taking into account multimagnon contributions within the SCBA. In this way we argue that the spin fluctuations play an essential role in the hole's dynamics. In particular the width of E_{QP} is determined by the nearest-neighbor spin exchange J.

II. SPIN-FERMION MODEL AND THE ONE-BAND MODEL DERIVED FROM IT

We start from the spin-fermion model (Cu spins and O holes), obtained from H_{3b} integrating out valence fluctuations at the Cu sites [8–10,23]. With an adequate choice of phases (see the Supplemental Material of Ref. [28]) the Hamiltonian reads

$$H_{sf} = \sum_{i\delta\delta'\sigma} p^{\dagger}_{i+\delta'\sigma} p_{i+\delta\sigma} \left[\left(t_1^{sf} + t_2^{sf}\right)\left(\frac{1}{2} + 2\mathbf{S}_i \cdot \mathbf{s}_{i+\delta}\right) - t_2^{sf} \right] - t_{pp} \sum_{j\gamma\sigma} p^{\dagger}_{j+\gamma\sigma} p_{j\sigma} + t'_{pp} \sum_{j\delta\sigma} (p^{\dagger}_{i+\delta\sigma} p_{i-\delta\sigma} + \text{H.c.}) - \sum_{i\delta} J_d \mathbf{S}_i \cdot \mathbf{s}_{i+\delta} + \frac{J}{2} \sum_{i\delta} \mathbf{S}_i \cdot \mathbf{S}_{i+2\delta}, \quad (1)$$

where i (j) labels the Cu (O) sites, $i+\delta$ ($j+\gamma$) label the four O atoms nearest Cu atom i (O atom j), and $p^{\dagger}_{j\sigma}$ creates an O hole at the $2p_\sigma$ orbital of site j with spin σ. The spin at the Cu site i (O orbital $2p_\sigma$ at site $i+\delta$) is denoted $\mathbf{S}_i$ ($\mathbf{s}_{i+\delta}$). As in Ref. [23], we include hopping t'_{pp} between second-neighbor O orbitals with a Cu in between, and we add J_d (which reduces part of the first term for $\delta' = \delta$), which was not included in earlier studies. The model is represented in Fig. 1. In units of the Cu-Cu spin exchange $J = 1$, the parameters chosen for the multiband model of Ref. [23] are $t_1^{sf} = 2.98$, $t_2^{sf} = 0$, $t_{pp} = 4.13$, $t'_{pp} = 2.40$, and $J_d = 3.13$. These parameters are near those calculated by constrained-density-functional calculations for La_2CuO_4 [48].

Projecting the Hamiltonian over the subspace of ZRSs, we have derived a one-band generalized t-J model:

$$H_{GtJ} = -\sum_{\kappa} t_\kappa \sum_{i v_\kappa \sigma} (c^{\dagger}_{i\sigma} c_{i+v_\kappa\sigma} + \text{H.c.}) + \frac{J}{2} \sum_{i v_1} \mathbf{S}_i \cdot \mathbf{S}_{i+v_1}, \quad (2)$$

where $c^{\dagger}_{i\sigma}$ creates a hole at the Cu site i with spin σ and $\kappa = 1, 2, 3$ refer to first-, second-, and third-nearest neighbors v_κ within the sublattice of Cu atoms. Additional terms are small and do not affect the hole dynamics. The derivation of this one-band Hamiltonian and the calculation of its parameters follow the procedure detailed in the Supplemental Material of Ref. [28], here generalized to include the effect of second-nearest-neighbor O hopping t'_{pp}. The contribution of this term for a hopping τ_R between sites at a distance $R = (x, y)$ becomes

$$\tau_R = \frac{2t'_{pp}}{N} \sum_k \cos(k_x x)\cos(k_y y) \times \left(1 - \frac{\cos^4(k_x b) + \cos^4(k_y b)}{\cos^2(k_x b) + \cos^2(k_y b)}\right), \quad (3)$$

where $b = a/2$ is half the lattice parameter and N is the number of sites of the cluster. The contribution of the other terms of H_{sf} to the different terms of H_{GtJ} was described in detail before [28]. The resulting parameters of H_{GtJ} are, taking $J = 0.15$ eV to be the unit of energy, $t_1 = 1.921$, $t_2 = -0.371$, $t_3 = 0.592$.

III. TREATMENT OF THE ONE-BAND MODEL

We calculate the QP spectral functions—from which the single hole's dispersion and weight are directly derived—and the magnon contributions to the hole's wave function (WF) by means of the SCBA [37,47,49,50], a semianalytic method that compares very well with exact diagonalization results on small clusters in different systems [37,47,50–52]. We must warn the reader that this approach has some limitations for $J/t_1 > 1$ [39,53]; however, in our case $J/t_1 \simeq 0.5$.

The SCBA is one of the most reliable and checked methods to date to calculate the hole Green's function, in particular, its QP dispersion relation. However, some care is needed to map the QP weight between different models [47]. In order to do such a calculation, we follow standard procedures [37]. On the one hand, the magnon dispersion relation is obtained by treating the magnetic part of the Hamiltonian at the linear spin-wave level since the system we study has long-range antiferromagnetic order, and it is well known that its magnetic excitations are semiclassical magnons [54]. On the other hand, the electron creation and annihilation operators in the hopping terms are mapped into holons of a slave-fermion representation (details in Ref. [28]). Within SCBA, we arrive at an effective Hamiltonian:

$$H_{\text{eff}} = \sum_{\mathbf{k}} \epsilon_{\mathbf{k}} h^{\dagger}_{\mathbf{k}} h_{\mathbf{k}} + \sum_{\mathbf{k}} \omega_{\mathbf{k}} \alpha^{\dagger}_{\mathbf{k}} \alpha_{\mathbf{k}} + \frac{1}{\sqrt{N}} \sum_{\mathbf{kq}} (M_{\mathbf{kq}} h^{\dagger}_{\mathbf{k}} h_{\mathbf{k-q}} \alpha_{\mathbf{q}} + \text{H.c.}), \quad (4)$$

with

$$\epsilon_{\mathbf{k}} = 4t_2\cos(ak_x)\cos(ak_y) + 2t_3[\cos(2ak_x) + \cos(2ak_y)],$$

$$\omega_{\mathbf{k}} = \sqrt{A_{\mathbf{k}}^2 - 4B_{\mathbf{k}}^2},$$

$$M_{\mathbf{kq}} = 2t_1[u_{\mathbf{q}}\zeta(\mathbf{k}-\mathbf{q}) - v_{\mathbf{q}}\zeta(\mathbf{k})], \quad (5)$$

where $\epsilon_{\mathbf{k}}$ is the bare hole dispersion (with no coupling to magnons); $\omega_{\mathbf{k}}$ is the magnon dispersion relation, with $A_{\mathbf{k}} = 2J$, $B_{\mathbf{k}} = \frac{J}{4}\sum_{\mathbf{R}}\cos(\mathbf{R}\cdot\mathbf{k})$; and $M_{\mathbf{kq}}$ is the vertex that couples the hole with magnon excitations. Here $\zeta(\mathbf{k}) = \cos(ak_x) + \cos(ak_y)$, where a is the distance between Cu atoms in the CuO_2 planes and $u_{\mathbf{q}}$ and $v_{\mathbf{q}}$ are the usual Bogoliubov coefficients, $u_{\mathbf{q}} = [(1+\nu_{\mathbf{q}})/2\nu_{\mathbf{q}}]^{1/2}$, $v_{\mathbf{q}} = -\mathrm{sgn}(\gamma_{\mathbf{q}})[(1-\nu_{\mathbf{q}})/2\nu_{\mathbf{q}}]^{1/2}$, with $\gamma_{\mathbf{q}} = \zeta(\mathbf{q})/2$.

The heart of the SCBA method lies in the self-consistent Dyson equation for the hole's self-energy [36],

$$\Sigma_{\mathbf{k}}(\omega) = \frac{1}{N}\sum_{\mathbf{q}}|M_{\mathbf{kq}}|^2 G_{\mathbf{k}-\mathbf{q}}(\omega - \omega_{\mathbf{q}}),$$

where $G_{\mathbf{k}}(\omega) = [\omega - \epsilon_{\mathbf{k}} - \Sigma_{\mathbf{k}}(\omega)]^{-1}$ is the hole Green's function. From the self-energy the QP energy can be computed by means of the self-consistent equation $E_{\mathrm{QP}}(\mathbf{k}) = \Sigma_{\mathbf{k}}[E_{\mathrm{QP}}(\mathbf{k})]$ and also the holon spectral weight, defined as [36]

$$Z_h(\mathbf{k}) = \left(1 - \frac{\partial \mathrm{Re}\ \Sigma_{\mathbf{k}}(\omega)}{\partial\omega}\right)^{-1}\Bigg|_{E_{\mathrm{QP}}(\mathbf{k})}. \quad (6)$$

Although Eq. (6), in principle, allows the calculation of the spectral weight directly, in practice within the SCBA it is impossible to apply it due to the strong irregularities in the derivative of $\mathrm{Re}\Sigma_{\mathbf{k}}$. Instead, the spectral weight is calculated by integrating the QP peak in the spectral function.

A. QP spectral function and magnon coefficients of the QP wave function

For the calculation of the magnon contributions to the QP's WF we follow the steps taken in Refs. [55–57]. The QP WF with momentum $\mathbf{k}$ can be expressed as a sum of terms, each of which involves the contribution of a growing number of magnons. Hence, within the SCBA, the QP WF results by taking the $n \to \infty$ limit of

$$|\Phi_{\mathbf{k}}^n\rangle = Z_h(\mathbf{k})\Bigg[h_{\mathbf{k}}^\dagger + \frac{1}{\sqrt{N}}\sum_{\mathbf{q}_1} g_{\mathbf{k},\mathbf{q}_1} h_{\mathbf{k}-\mathbf{q}_1}^\dagger \alpha_{\mathbf{q}_1}^\dagger + \cdots + \frac{1}{\sqrt{N^n}}\sum_{\mathbf{q}_1,\ldots,\mathbf{q}_n} g_{\mathbf{k},\mathbf{q}_1} g_{\mathbf{k}_1,\mathbf{q}_2}\cdots g_{\mathbf{k}_{n-1},\mathbf{q}_n} h_{\mathbf{k}_n}^\dagger \alpha_{\mathbf{q}_1}^\dagger\cdots\alpha_{\mathbf{q}_n}^\dagger\Bigg]|\mathrm{AF}\rangle,$$

where $\mathbf{k}_i = \mathbf{k} - \mathbf{q}_1 - \cdots - \mathbf{q}_i$, $|\mathrm{AF}\rangle$ is the undoped antiferromagnetic ground state, and

$$g_{\mathbf{k}_n,\mathbf{q}_{n+1}} = M_{\mathbf{k}_n,\mathbf{q}_{n+1}} G_{\mathbf{k}_{n+1}}[E_{\mathrm{QP}}(\mathbf{k}) - \omega_{\mathbf{q}_1} - \cdots - \omega_{\mathbf{q}_{n+1}}]. \quad (7)$$

It can be seen that each contributing term to the QP WF involves a growing number of magnons, starting from the first zero magnon term whose relative weight is given by the holon spectral weight $Z_h(\mathbf{k})$.

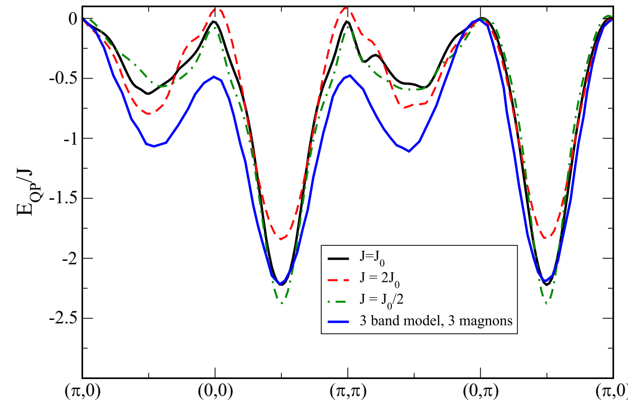

FIG. 2. QP hole dispersion relation. The solid black (blue) curve corresponds to the QP dispersion relation for the one-band generalized t-J model (three-band model) calculated with SCBA (the variational approach). The dashed red (dash-dotted green) curve corresponds to the SCBA QP dispersion for a one-band model with an exchange interaction twice (half) the value of the experimental one.

The QP WF satisfies the normalization condition

$$S_{\mathbf{k}} = \lim_{n\to\infty}\langle\Phi_{\mathbf{k}}^n|\Phi_{\mathbf{k}}^n\rangle = \sum_{m=0}^{\infty} A_{\mathbf{k}}^{(m)} = 1. \quad (8)$$

Each coefficient $A_{\mathbf{k}}^{(m)}$ is the m-magnon contribution to the QP WF and is defined as

$$A_{\mathbf{k}}^{(m)} = \frac{z_{\mathbf{k}}}{N^m}\sum_{\mathbf{q}_1,\ldots,\mathbf{q}_n} g_{\mathbf{k},\mathbf{q}_1}^2 g_{\mathbf{k}_1,\mathbf{q}_2}^2\cdots g_{\mathbf{k}_{m-1},\mathbf{q}_m}^2, \quad (9)$$

while for the particular case $m = 0$, $A_{\mathbf{k}}^{(0)} \equiv Z_h(\mathbf{k})$. In this way, within the SCBA the relative weight of each n-magnon term for the spin polaron can be evaluated for a specific moment of the Brillouin zone.

In order to estimate the effective number of magnons necessary to have a reliable QP WF we can find the minimum n such that $S_{\mathbf{k}}^{(n)} = \langle\Phi_{\mathbf{k}}^n|\Phi_{\mathbf{k}}^n\rangle = \sum_{m=0}^{n} A_{\mathbf{k}}^{(m)} \simeq 1$, within a certain precision.

IV. RESULTS

In this section we present the SCBA calculations for $H_{G\,t-J}$, using the previously estimated parameters and the experimental value $J \equiv J_0 = 0.15$ eV.

A. Quasiparticle dispersion relation

Figure 2 shows the SCBA QP dispersion relation corresponding to our one-band generalized t-J model along with the QP dispersion relation of the three-band model, obtained variationally [24]. We recall that in our model there are no free parameters. All of them are rigorously obtained from the three-band model [23] and experiments. The agreement of the one-band model and the multiband model dispersions is very good near the QP ground state momentum $(\frac{\pi}{2}, \frac{\pi}{2})$ and all along the diagonal and antidiagonal lines. In the rest of the chosen path, the agreement is semiquantitative. Compared with the ARPES measurements [34,58], our results seem to better capture the quasidegeneracy between the (π, π) and $(\pi, 0)$ points, with the energy at $(\pi, 0)$ a little higher than

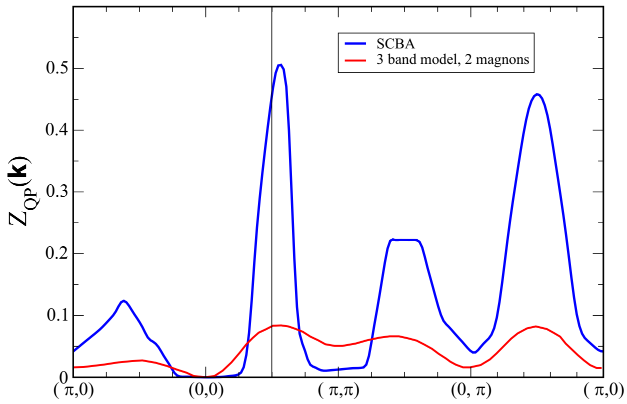

FIG. 3. QP spectral weight: the blue curve corresponds to the O contribution to the photoemission intensity calculated with SCBA, while the red curve corresponds to the QP weight function of the three-band model calculated variationally (taken from Ref. [23]).

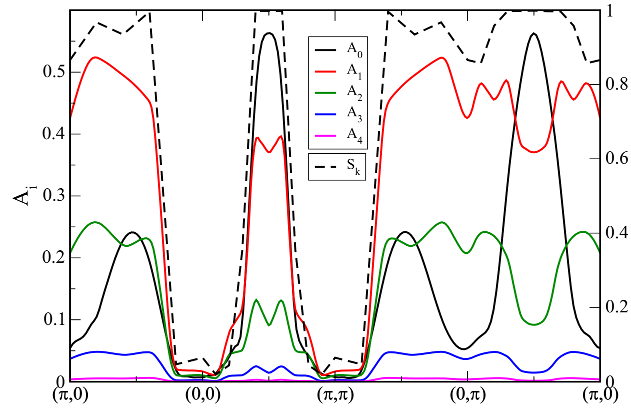

FIG. 4. Solid curves: Magnon coefficients $A_{\mathbf{k}}^{(m)}$ of the SCBA QP wave function for $N = 400$. Dashed curve: sum of the first four magnon coefficients.

that at (π, π). It should be stressed that, for simplicity, we are taking a hole picture, so the dispersion relation should be reversed in order to be compared with ARPES. From only the dispersion relation, it is not possible to conclusively discern whether the SCBA solution of the generalized t-J model or the variational solution of the three-band model predictions agrees better with ARPES.

To analyze the role of the spin fluctuations for the hole motion within our theory, we also plot in Fig. 2 the SCBA QP dispersion relation for the same H_{GtJ} parameters but half and double exchange interaction J values. The first point to notice is that as a first approximation, the bandwidth is directly proportional to J. When $J = 2J_0$, that is, the spin fluctuations are enhanced in comparison with the hole kinetic energy, the relative dispersion bandwidth (in units of the corresponding J) is decreased, and now the energy of the $\mathbf{k} = (0, 0)$ and (π, π) points is slightly higher than that at the $(\pi, 0)$ point, in contrast to ARPES. On the other hand, the dispersion for $J = J_0/2$, i.e., when spin fluctuations are lowered, has the same structure as for $J = J_0$, but its relative bandwidth is larger than that of the three-band model. Therefore, it is evident that the spin fluctuations have a noticeable impact on the global dispersion form and its bandwidth. In particular, the increase of the exchange interaction gives rise to more localized QP states.

In previous treatments of the spin-fermion model the QP dispersion relation was found to be qualitatively similar for Ising and Heisenberg backgrounds [23,24]. We believe that the lack of a discrepancy is most likely attributable to the variational treatment lacking enough magnons.

B. Quasiparticle spectral weight

In Fig. 3 we show the QP spectral weight for the one-band and three-band models along the same Brillouin zone path as in Fig. 2. Care must be taken to calculate the QP spectral weight within the one-band model since almost all of the contribution to the photoemission spectra comes from the addition of an O hole. However, in the one-band model the O degrees of freedom have been integrated. In order to compute the O contribution to the ARPES QP intensity $Z_{QP}(\mathbf{k})$ within the SCBA, we follow the procedures of Ref. [43]: we first calculate the *holon* spectral weight $Z_h(\mathbf{k})$, we then calculate the spectral weight for emitting a *physical* electron (see Ref. [47]), and finally, from this we calculate the O intensity by means of a simple analytical relation between both, as detailed in Ref. [43]. In general, the calculated O intensity is higher than that of the variational calculation of the three-band model. Even so, it can be seen that along the diagonal $(0, 0) \rightarrow (\pi, \pi)$, the intensity is large near the ground state $(\pi/2, \pi/2)$ momentum [note that it is not symmetric around $(\pi/2, \pi/2)$], but it decreases abruptly when approaching both (0,0) and (π, π). Nevertheless, these momenta do not show degeneracy in the intensity, which happens for the holon weight within the SCBA [37].

The general trend of the intensity calculated with the generalized t-J model by means of the SCBA coincides with experiments [34,58], in contrast to the results of the variational three-band model calculations [23]. In particular, the experiments show an almost vanishing QP photoemission weight close to (0,0) and (π, π) (see Fig. 1 of Ref. [34]) that is correctly captured by our results, while in the three-band model calculation the (π, π) point has an appreciable QP weight. Reference [23] showed that using a five-band model a partial decrease of the QP weight is obtained at (π, π), while our more sophisticated SCBA calculation already captures this spectral feature in the one-band generalized t-J model. Hence, we believe that the one-band model provides a quantitatively correct description of the photoemission spectra for the undoped cuprates.

C. Magnon contributions to the QP wave function

In Fig. 4 we show the magnon coefficients $A_{\mathbf{k}}^{(m)}$ for $m = 1, 2, 3$, and 4, along the same path in the Brillouin zone as in Fig. 2. The data shown were obtained for a cluster of $N = 400$ sites using 25 000 frequencies. We have checked that the results are essentially the same as for $N = 1600$ sites, which is an indication that the $N = 400$ cluster is a very good approximation for the thermodynamic limit. We have chosen this cluster size because, for 1600 sites, the calculation of the fourth coefficient $A_{\mathbf{k}}^{(4)}$ is computationally expensive. For

TABLE I. Magnon coefficients $A_{\mathbf{k}}^{(m)}$ for $m = 1, 2, 3$ calculated for an $N = 1600$ cluster for selected momenta along the diagonal of the Brillouin zone. By symmetry, $A^{(m)}_{(\frac{\pi}{2}+k,\frac{\pi}{2}+k)} = A^{(m)}_{(\frac{\pi}{2}-k,\frac{\pi}{2}-k)}$.

k_x/π	k_y/π	$A_{\mathbf{k}}^{(0)}$	$A_{\mathbf{k}}^{(1)}$	$A_{\mathbf{k}}^{(2)}$	$A_{\mathbf{k}}^{(3)}$	$S_{\mathbf{k}}$
0.0	0.0	0.0048	0.0055	0.0032	0.00073	0.014
0.1	0.1	0.0059	0.0080	0.0044	0.00095	0.019
0.2	0.2	0.012	0.021	0.011	0.0023	0.047
0.3	0.3	0.056	0.086	0.041	0.0087	0.19
0.4	0.4	0.42	0.40	0.15	0.029	0.99
0.5	0.5	0.55	0.38	0.10	0.017	1.00

comparison, we put in Table I the $A^{(m)}$ $m = 1, 2, 3$ coefficients for the 1600 cluster and for selected momenta along the diagonal $(0, 0) - (\pi, \pi)$. It is worth mentioning that for a correct computation of all the magnon coefficients it is essential to get a very precise QP dispersion relation and its spectral weight, as can be seen from Eqs. (7) and (9). For this purpose, it is necessary to use a very large number of frequencies.

What can be clearly seen in Fig. 4 and Table I is that the one- and two-magnon coefficients can be, for many momenta, greater than or of the same order of magnitude as the zero-magnon coefficient $A_{\mathbf{k}}^{(0)}$, which we recall is the holon spectral weight $Z_h(\mathbf{k})$. The three-magnon coefficient $A^{(3)}$ is small for all momenta but is by no means negligible. On the other hand, $A_{\mathbf{k}}^{(4)}$ is always very small, even compared to $A_{\mathbf{k}}^{(3)}$. From the magnon coefficients it can be concluded that spin fluctuations corresponding to several magnons are essential to build up the QP wave function. Since our one-band generalized t-J model is rigorously derived from a multiband model and, as we have shown above, it reproduces the main features of the experimental QP dispersion relation and photoemission intensity, it can be stated that the spin polaron [37] is the appropriate physical picture of the QP in cuprates. In this sense, other points of view have been proposed, such as the string picture [59] and the parton theory [60], all of which support the importance of spin fluctuations in the physics of cuprate superconductors.

Figure 4 also displays the partial sum of the norm $S_{\mathbf{k}}^{(4)}$, which is the sum of the first four magnon coefficients. It is evident that for those momenta where the holon QP weight $Z_h(\mathbf{k})$ is not so small ($Z_h \gtrsim 0.05$), the normalization rule (8) is reasonably satisfied with only a very few magnon coefficients. If the sum does not reach the value 1, it is very close, and hence, it can be argued that with the inclusion of a few more magnon coefficients, the condition would be fulfilled. In this case, the QP can be thought of as the bare hole moving around, exciting up to only three or four magnons. On the other hand, it is also clear that close to $\mathbf{k} = (0, 0)$ and (π, π), where the holon QP spectral weight is much smaller than 0.05, the normalization condition is far from being satisfied. Since the four-magnon coefficients $A_{\mathbf{k}}^{(4)}$ are much smaller than the three-magnon ones $A_{\mathbf{k}}^{(3)}$, it is plausible to assume that the following coefficients would be even smaller, and so there must be a "magnon proliferation"; that is, the QP would be composed of a great number of magnons, and the sum rule can be reasonably satisfied only with a huge number of magnon coefficients, corresponding to very slowly convergent series.

In the pure t-J model ($t_2 = t_3 = 0$), for a J/t ratio like our J/t_1, Ramšak and Horsch [56] showed that the QP is also composed of several magnons, that for some momenta the one-magnon coefficient is larger than the zero-magnon one, and even that the two- and three-magnon terms are important to fulfill the normalization condition. This behavior is analogous to the one we have found in this work. However, it is known that in the pure t-J model the hole can propagate only by emitting and absorbing spin fluctuations [36]. In addition, this model does not reproduce the experimentally measured dispersion [34]. With our generalized model, with second- and third-nearest-neighbor hoppings, we were able to reproduce the experiments. It is usually argued [23] that, since t_2 and t_3 allow free hopping processes, in which the hole can move along a magnetic sublattice without disturbing the Néel order, the correct dispersion obtained by including further hoppings in the model implies that spin fluctuations do not play an important role in the QP formation. Our results indicate that this is not the case and that for the generalized H_{Gt-J} the multimagnon processes are equally important in the formation of the QP as in the pure t-J model. In previous works [51,52] we already showed that even when there is a "free hopping" channel that allows the hole to move without generating spin fluctuations of the magnetic background, the hole motion is promoted by emitting magnons since this is, all in all, energetically favorable.

V. CONCLUSIONS

Recent variational calculations [23,24,27] have suggested that one-band models cannot give a correct description of cuprate superconductors based on the argument that these models, without *ad hoc* terms, fail to describe even the ARPES photoemission spectra for a hole doped into an antiferromagnetically ordered CuO_2 layer. Also, these works argue that the spin polaron nature of a single hole doped in undoped cuprates is different in one- and multiband models. To elucidate these claims, in this work we have performed a rigorous derivation of a one-band Zhang-Rice singlet based generalized t-J model for cuprate superconductors, with no free parameters, starting from a three-band model. Its hopping terms, appreciable up to third-nearest neighbors, are obtained from the three-band model parameters [23], while the exchange interaction J between copper sites is taken from experimental measurements.

With the well-established SCBA, we have computed the QP dispersion relation and the oxygen contribution to the photoemission intensity, obtaining satisfactory agreement with ARPES experiments [34,58], improving the above-mentioned variational three-band model calculations [23]. Particularly, we have reproduced the experimental abrupt drop of the QP spectral weight going away from $(\frac{\pi}{2}, \frac{\pi}{2})$ to (π, π) that, within the variational calculation, can be only partially obtained using a more complicated five-band model.

In addition, we have analyzed the structure of the SCBA QP wave function computing its magnon coefficients, and we have found that the spin fluctuations play an essential role in the building up of the QP. This happens even for our generalized t-J model in which second- and third-nearest-neighbor hoppings allow the hole motion without emitting magnon excitations of the antiferromagnetic background.

From our results we can conclude that rigorously derived one-band models are appropriate for the description of the low-energy physics of (at least slightly doped) cuprate superconductors, while the physical nature of a single hole doped in a CuO_2 layer corresponds to a spin polaron quasiparticle with spin fluctuations as its main ingredient.

ACKNOWLEDGMENTS

I.J.H. and L.O.M. are partially supported by Grant No. PIP 0364 of CONICET, Argentina. A.A.A. is sponsored by Grant No. PIP 112-201501-00506 of CONICET and Grants No. PICT 2017-2726 and No. PICT 2018-01546 of ANPCyT, Argentina.

[1] V. J. Emery, Theory of High-T_c Superconductivity in Oxides, Phys. Rev. Lett. **58**, 2794 (1987).
[2] C. M. Varma, S. Schmitt-Rink, and E. Abrahams, Charge transfer excitations and superconductivity in "ionic" metals, Solid State Commun. **62**, 681 (1987).
[3] R. Raimondi, J. H. Jefferson, and L. F. Feiner, Effective single-band models for the high-t_c cuprates. II. Role of apical oxygen, Phys. Rev. B **53**, 8774 (1996).
[4] M. E. Simón, A. A. Aligia, C. D. Batista, E. R. Gagliano, and F. Lema, Excitons in insulating cuprates, Phys. Rev. B **54**, R3780(R) (1996).
[5] M. Jiang, M. Moeller, M. Berciu, and G. A. Sawatzky, Relevance of Cu–3d multiplet structure in models of high-T_c cuprates, Phys. Rev. B **101**, 035151 (2020).
[6] S. Acharya, C. Weber, E. Plekhanov, D. Pashov, A. Taraphder, and M. Van Schilfgaarde, Metal-Insulator Transition in Copper Oxides Induced by Apex Displacements, Phys. Rev. X **8**, 021038 (2018).
[7] F. Jamet, C. Weber, S. Acharya, D. Pashov, and M. van Schilfgaarde, Disentangling the role of bond lengths and orbital symmetries in controlling t_c in $YBa_2Cu_3O_7$, arXiv:2012.04897.
[8] V. J. Emery and G. Reiter, Quasiparticles in the copper-oxygen planes of high-T_c superconductors: An exact solution for a ferromagnetic background, Phys. Rev. B **38**, 11938 (1988).
[9] C. Batista and A. A. Aligia, Validity of the t-j model: Quantum numbers for $(Cu_4O_8)^{-7}$, Solid State Commun. **83**, 419 (1992).
[10] C. D. Batista and A. A. Aligia, Effective Hamiltonian for cuprate superconductors, Phys. Rev. B **47**, 8929 (1993).
[11] F. C. Zhang and T. M. Rice, Effective Hamiltonian for the superconducting Cu oxides, Phys. Rev. B **37**, 3759 (1988).
[12] A. A. Aligia, M. E. Simón, and C. D. Batista, Systematic derivation of a generalized t-j model, Phys. Rev. B **49**, 13061 (1994).
[13] V. I. Belinicher, A. L. Chernyshev, and L. V. Popovich, Range of the t-j model parameters for CuO_2 planes: Experimental data constraints, Phys. Rev. B **50**, 13768 (1994), and references therein.
[14] L. F. Feiner, J. H. Jefferson, and R. Raimondi, Effective single-band models for the high-T_c cuprates. I. Coulomb interactions, Phys. Rev. B **53**, 8751 (1996).
[15] A. A. Aligia, Comment on Relevance of Cu-3d multiplet structure in models of high-T_c cuprates, Phys. Rev. B **102**, 117101 (2020).
[16] F. C. Zhang, Exact mapping from a two-band model for Cu oxides to the single-band Hubbard model, Phys. Rev. B **39**, 7375 (1989).
[17] H.-Q. Ding, G. H. Lang, and W. A. Goddard, Band structure, magnetic fluctuations, and quasiparticle nature of the two-dimensional three-band Hubbard model, Phys. Rev. B **46**, 14317 (1992).
[18] C. D. Batista and A. A. Aligia, Validity of the t-j model, Phys. Rev. B **48**, 4212 (1993).
[19] L.-C. Duda, J. Downes, C. McGuinness, T. Schmitt, A. Augustsson, K. E. Smith, G. Dhalenne, and A. Revcolevschi, Bandlike and excitonic states of oxygen in $CuGeO_3$: Observation using polarized resonant soft-x-ray emission spectroscopy, Phys. Rev. B **61**, 4186 (2000).
[20] B. Lau, M. Berciu, and G. A. Sawatzky, High-Spin Polaron in Lightly Doped CuO_2 Planes, Phys. Rev. Lett. **106**, 036401 (2011).
[21] L. de' Medici, X. Wang, M. Capone, and A. J. Millis, Correlation strength, gaps, and particle-hole asymmetry in high-T_c cuprates: A dynamical mean field study of the three-band copper-oxide model, Phys. Rev. B **80**, 054501 (2009).
[22] W.-C. Lee and T. K. Lee, Comment on High-spin polaron in lightly doped CuO_2 planes, arXiv:1108.5413.
[23] H. Ebrahimnejad, G. A. Sawatzky, and M. Berciu, The dynamics of a doped hole in a cuprate is not controlled by spin fluctuations, Nat. Phys. **10**, 951 (2014).
[24] H. Ebrahimnejad, G. A. Sawatzky, and M. Berciu, Differences between the insulating limit quasiparticles of one-band and three-band cuprate models, J. Phys.: Condens. Matter **28**, 105603 (2016).
[25] N. B. Brookes, G. Ghiringhelli, A.-M. Charvet, A. Fujimori, T. Kakeshita, H. Eisaki, S. Uchida, and T. Mizokawa, Stability of the Zhang-Rice Singlet with Doping in Lanthanum Strontium Copper Oxide Across the Superconducting Dome and Above, Phys. Rev. Lett. **115**, 027002 (2015).
[26] A. Chainani, M. Sicot, Y. Fagot-Revurat, G. Vasseur, J. Granet, B. Kierren, L. Moreau, M. Oura, A. Yamamoto, Y. Tokura, and D. Malterre, Evidence for Weakly Correlated Oxygen Holes in the Highest-T_c Cuprate Superconductor $HgBa_2Ca_2Cu_3O_{8+\delta}$, Phys. Rev. Lett. **119**, 057001 (2017).
[27] C. P. J. Adolphs, S. Moser, G. A. Sawatzky, and M. Berciu, Non-Zhang-Rice Singlet Character of the First Ionization State of T-CuO, Phys. Rev. Lett. **116**, 087002 (2016).
[28] I. J. Hamad, L. O. Manuel, and A. A. Aligia, Generalized One-Band Model Based on Zhang-Rice Singlets for Tetragonal Cuo, Phys. Rev. Lett. **120**, 177001 (2018).
[29] A. Greco, Evidence for Two Competing Order Parameters in Underdoped Cuprate Superconductors from a Model Analysis of Fermi-Arc Effects, Phys. Rev. Lett. **103**, 217001 (2009), and references therein.
[30] A. Greco, H. Yamase, and M. Bejas, Origin of high-energy charge excitations observed by resonant inelastic x-ray scattering in cuprate superconductors, Commun. Phys. **2**, 3 (2019).
[31] C. D Batista, L. O Manuel, H. A Ceccatto, and A. A Aligia, Superconductivity and incommensurate spin fluctuations in a

generalized t-j model for the cuprates, Europhys. Lett. **38**, 147 (1997).

[32] A. V. Mallik, G. K. Gupta, V. B. Shenoy, and H. R. Krishnamurthy, Surprises in the t-j Model: Implications for Cuprates, Phys. Rev. Lett. **124**, 147002 (2020).

[33] N. M. Plakida, Superconductivity in the t-j model, Condens. Matter Phys. **5**, 32 (2002).

[34] B. O. Wells, Z. X. Shen, A. Matsuura, D. M. King, M. A. Kastner, M. Greven, and R. J. Birgeneau, E Versus **k** Relations and Many Body Effects in the Model Insulating Copper Oxide $Sr_2CuO_2Cl_2$, Phys. Rev. Lett. **74**, 964 (1995).

[35] S. Moser, L. Moreschini, H.-Y. Yang, D. Innocenti, F. Fuchs, N. H. Hansen, Y. J. Chang, K. S. Kim, A. L. Walter, A. Bostwick, E. Rotenberg, F. Mila, and M. Grioni, Angle-Resolved Photoemission Spectroscopy of Tetragonal CuO: Evidence for Intralayer Coupling between Cupratelike Sublattices, Phys. Rev. Lett. **113**, 187001 (2014).

[36] C. L. Kane, P. A. Lee, and N. Read, Motion of a single hole in a quantum antiferromagnet, Phys. Rev. B **39**, 6880 (1989).

[37] G. Martinez and P. Horsch, Spin polarons in the t-j model, Phys. Rev. B **44**, 317 (1991).

[38] A. S. Mishchenko, N. V. Prokof'ev, and B. V. Svistunov, Single-hole spectral function and spin-charge separation in the t-j model, Phys. Rev. B **64**, 033101 (2001).

[39] M. Brunner, F. F. Assaad, and A. Muramatsu, Single-hole dynamics in the t-j model on a square lattice, Phys. Rev. B **62**, 15480 (2000).

[40] N. Nücker, H. Romberg, X. X. Xi, J. Fink, B. Gegenheimer, and Z. X. Zhao, Symmetry of holes in high-T_c superconductors, Phys. Rev. B **39**, 6619 (1989).

[41] M. Takigawa, P. C. Hammel, R. H. Heffner, Z. Fisk, K. C. Ott, and J. D. Thompson, ^{17}O NMR Study of Local Spin Susceptibility in Aligned $YBa_2Cu_3O_7$ Powder, Phys. Rev. Lett. **63**, 1865 (1989).

[42] M. Oda, C. Manabe, and M. Ido, STM images of a superconducting Cu-O plane and the corresponding tunneling spectrum in $Bi_2Sr_2CaCu_2O_{8+\delta}$, Phys. Rev. B **53**, 2253 (1996).

[43] J. Eroles, C. D. Batista, and A. A. Aligia, Angle-resolved Cu and O photoemission intensities in CuO_2 planes, Phys. Rev. B **59**, 14092 (1999).

[44] A. Nazarenko, K. J. E. Vos, S. Haas, E. Dagotto, and R. J. Gooding, Photoemission spectra of $Sr_2CuO_2Cl_2$: A theoretical analysis, Phys. Rev. B **51**, 8676 (1995).

[45] T. Xiang and J. M. Wheatley, Quasiparticle energy dispersion in doped two-dimensional quantum antiferromagnets, Phys. Rev. B **54**, R12653(R) (1996).

[46] V. I. Belinicher, A. L. Chernyshev, and V. A. Shubin, Single-hole dispersion relation for the real CuO_2 plane, Phys. Rev. B **54**, 14914 (1996).

[47] F. Lema and A. A. Aligia, Quasiparticle photoemission intensity in doped two-dimensional quantum antiferromagnets, Phys. Rev. B **55**, 14092 (1997).

[48] M. S. Hybertsen, M. Schlüter, and N. E. Christensen, Calculation of Coulomb-interaction parameters for La_2CuO_4 using a constrained-density-functional approach, Phys. Rev. B **39**, 9028 (1989).

[49] F. Lema and A. A. Aligia, Spectral function and quasiparticle weight in the generalized t-j model, Physica C (Amsterdam, Neth.) **307**, 307 (1998).

[50] A. E. Trumper, C. J. Gazza, and L. O. Manuel, Quasiparticle vanishing driven by geometrical frustration, Phys. Rev. B **69**, 184407 (2004).

[51] I. J. Hamad, A. E. Trumper, A. E. Feiguin, and L. O. Manuel, Spin polaron in the J_1-J_2 Heisenberg model, Phys. Rev. B **77**, 014410 (2008).

[52] I. J. Hamad, L. O. Manuel, and A. E. Trumper, Effects of semiclassical spiral fluctuations on hole dynamics, Phys. Rev. B **85**, 024402 (2012).

[53] P. Wrzosek and K. Wohlfeld, Hole in the two-dimensional Ising antiferromagnet: Origin of the incoherent spectrum, Phys. Rev. B **103**, 035113 (2021).

[54] R. Coldea, S. M. Hayden, G. Aeppli, T. G. Perring, C. D. Frost, T. E. Mason, S.-W. Cheong, and Z. Fisk, Spin Waves and Electronic Interactions in La_2CuO_4, Phys. Rev. Lett. **86**, 5377 (2001).

[55] G. F. Reiter, Self-consistent wave function for magnetic polarons in the t-j model, Phys. Rev. B **49**, 1536 (1994).

[56] A. Ramšak and P. Horsch, Spatial structure of spin polarons in the t-j model, Phys. Rev. B **57**, 4308 (1998).

[57] A. E. Trumper, C. J. Gazza, and L. O. Manuel, Quasiparticle excitations in frustrated antiferromagnets, Physica B (Amsterdam, Neth.) **354**, 252 (2004).

[58] A. Damascelli, Z. Hussain, and Z.-X. Shen, Angle-resolved photoemission studies of the cuprate superconductors, Rev. Mod. Phys. **75**, 473 (2003).

[59] E. Manousakis, String excitations of a hole in a quantum antiferromagnet and photoelectron spectroscopy, Phys. Rev. B **75**, 035106 (2007).

[60] A. Bohrdt, E. Demler, F. Pollmann, M. Knap, and F. Grusdt, Parton theory of angle-resolved photoemission spectroscopy spectra in antiferromagnetic Mott insulators, Phys. Rev. B **102**, 035139 (2020).